Flutter Suppression of a Bridge Section Model Endowed with Actively Controlled Flap Arrays

Maria Boberg, Glauco Feltrin and Alcherio Martinoli

***Abstract*— In this work, we investigate active flutter control of a bridge section model equipped with arrays of flaps. We consider three simple control algorithms based on an amplitude-gain and a phase-shift for actuating the flaps and stabilizing the section model. We have leveraged a linear analytical model of the structural and aeroelastic forces during flutter in order to find efficient control parameters. The proposed solution was validated with wind tunnel experiments, where all the algorithms showed capable of suppressing flutter, and the most efficient one was using all of the flaps on the deck.**

I. Introduction

Long-span bridges are particularly vulnerable to wind loads, owing to their inherently low structural damping, low natural frequencies, and adjacent fundamental torsional and vertical mode frequencies. This leads to wind-induced instabilities, causing potential damage to the whole structure.

Most solutions for this problem deployed on real bridges consist of passive elements that reduce the aerodynamic requirements on the cross-section [1]. However, a passive solution cannot adapt to dynamic wind conditions. Active solutions could potentially lead to a more favorable performance/cost trade-off in the building and maintenance phases as well as new opportunities for improving bridge aesthetics.

One possible active solution is to install multiple mobile flaps along the bridge girder in order to alter its aerodynamic profile, enabling stabilizing forces on the structure, a concept illustrated in Fig. 1. Furthermore, the angular position of the adjustable flaps is controlled as a function of the wind field and/or the displacement of the structure whose dynamic state can be measured with an underlying sensor network.

Several control strategies for moving flaps damping bridge deck oscillations have been investigated. In particular, the aeroelastic instability called flutter (causing self-induced vibrations), has been investigated. However, only a handful of research groups have provided experimental validation of bridge flutter control. Kobayashi et al. [2] managed to prevent flutter with actively controlled flaps installed above the bridge deck. Kobayashi et al. [3] followed up their work and also showed an efficient flutter control with flaps attached directly to the bridge deck, as in Fig. 1. Moreover, Hansen et al. [4, 5] also designed an active bridge deck capable of stabilizing the bridge vibrations, with actively controlled flaps attached to the deck. More recently, Zhao et al. [6] designed a controlled deck capable of suppressing flutter and buffeting.

Maria Boberg and Alcherio Martinoli are with the Distributed Intelligent Systems and Algorithms Laboratory, School of Architecture, Civil and Environmental Engineering, École Polytechnique Fédérale de Lausanne, Switzerland. maria.boberg@epfl.ch and alcherio.martinoli@epfl.ch

Maria Boberg and Glauco Feltrin are with the Structural Engineering Laboratory, Swiss Federal Laboratories for Materials Science and Technology, Duebendorf, Switzerland. glauco.feltrin@empa.ch

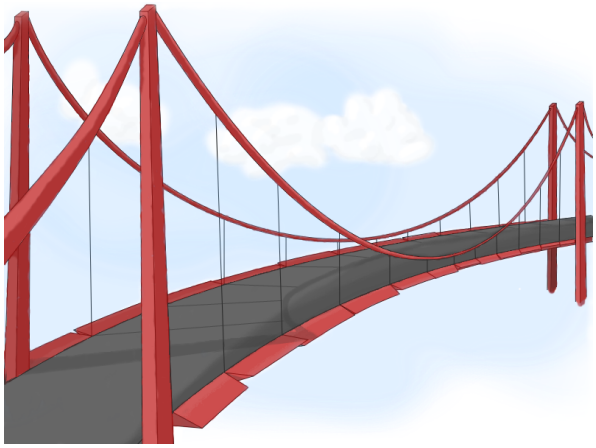

Fig. 1. Conceptual figure of the multi-flap wind mitigation strategy.

All of these research groups used bridge section models endowed with a single flap on each side of the girder. We aim to extend the investigation of active flutter control to bridge section models endowed with multiple flaps on each side, so that the potential of a physically distributed mitigation system can be studied and validated experimentally.

Kobayashi et al. [3] analyzed theoretically flap control using the bridge pitch, the deck heave and both Degrees of Freedom (DOFs) as control input for a linear amplitude-gain and phase-shift control law. However, they were only analyzing the effect of actuating the flaps separately, not simultaneously. Furthermore, the authors do not disclose how they chose the specific control parameters. The control algorithm that was found the most promising in theory was implemented and tested with wind tunnel experiments. Flutter suppression was achieved using only one of the flaps, the one on the trailing edge. Hansen et al. [4] also chose a linear amplitude-gain and phase-shift control law, using the bridge pitch as input. They conducted a thorough theoretical investigation of the controlled deck. The control parameters were found by maximizing the energy contribution of the flaps to the system. However, the obtained optimal control parameters, were not tested with wind tunnel experiments. Various amplitude-gain and phase-shift combinations were tested for different wind speeds; however, neither with the optimized parameters, nor for the flutter condition; thus, vibration control below the flutter regime was validated

experimentally. Zhao et al [6] proposed a passive mechanical controller concept (although realized with active control emulating a passive one). The trailing and leading edges were given the same control parameters, in order to achieve a symmetric design, insensitive to the wind direction. They designed a robust flutter controller for the passive mechanism, that achieved an increase in flutter wind speed both in theory and in practice.

All of the research groups leveraged the same analytical framework: the aerodynamic model based on Theodorsen's circulatory function for thin airfoils [7] and its extension with a modified version of the wing-aileron-tab configuration (transformed to apply to a bridge deck with leading and trailing flaps) developed by Theodorsen and Garrick [8]. The theory is however only valid close to the flutter frequency, where the system can be approximated as linear. Furthermore, the flaps are assumed to move at the same frequency as the bridge deck, thus the amplitude-gain and phase-shift control law is motivated in order to not violate the model assumptions.

In this work, we investigate, theoretically and experimentally, the amplitude-gain and phase-shift control law applied to the SmartBridge, our active bridge section model endowed with flap arrays. Although, the model is equipped with multiple flaps, we move all the flaps on both edges synchronized, so that they move as a single unison flap on each side of the deck. The experiments with synchronized flap movements are used to validate our approach and will serve as a baseline for future work involving fine-grained distributed control strategies of individual flaps. Nevertheless, in this paper we investigate a basic multi-flap coordination strategy by comparing the effect of the bridge deck control using only the leading edge flaps, only the trailing edge flaps, or all flaps on both sides of the deck.

Similar to our work presented in [9], where the control law of a single flap was optimized through a model-based approach, we are also in this work leveraging an analytical model to find appropriate control parameters. A model-based approach is particularly useful in the case of flutter control, as the effects of applying unfavorable control parameters can be catastrophic, [4]. The control algorithms found via the analytical investigation were validated through systematic wind tunnel experiments, and all three implemented control laws were capable of suppressing flutter, although with different performances.

II. Material and Methods

A. Experimental set-up

Our experimental set-up consists of the SmartBridge that is anchored to a suspension system as seen in Fig. 2. Note that the decoupling system seen in the figure has not been used for the work presented here. Instead, drag wires restrict the deck motions in the horizontal DOF. The SmartBridge is installed in a boundary layer wind tunnel, with channel dimensions of 1.5x2x10 m, and with a maximal wind speed set at 16 m/s. The parameters of the section model that are used in the analytical study are given in Table I, and were

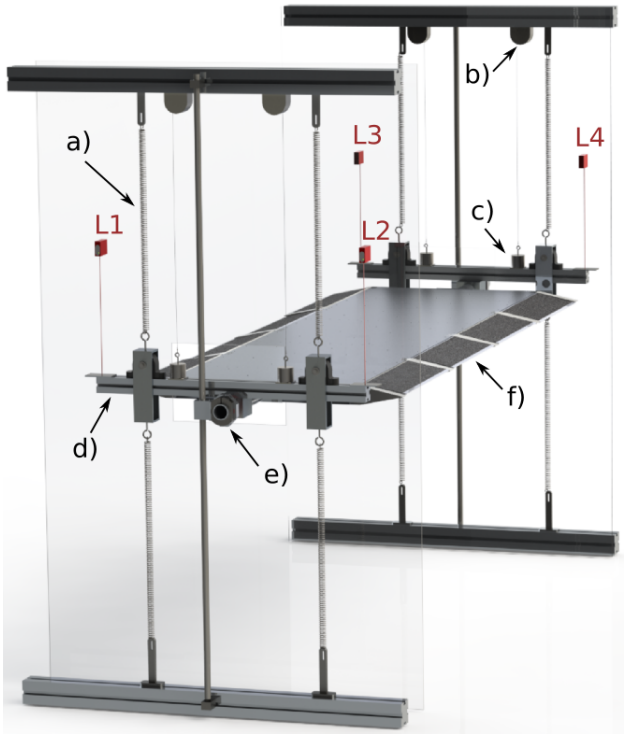

Fig. 2. A faithful CAD model of the SmartBridge anchored to the suspension system. Some key elements of the set up are highlighted in the figure: a) spring for the suspension system, b) DC motor for the pull-up system, c) electromagnet for the pull-up system, d) support bar, e) decoupling system, and f) active flap. Moreover, four laser sensors are measuring the corner positions of the deck and are marked with L1-4.

either measured directly from the model, or estimated from free vibration step responses using the pull-up system in Fig. 2. Further details of our experimental set-up and in particular the active bridge section model are presented in [10].

B. Analytical model of canonical bridge deck

The analytical model of the bridge section model is based on the heave and pitch DOFs, the two fundamental modes involved in coupled flutter. The two-dimensional model of the bridge deck and definitions of positive directions, are visualized in Fig. 3. Under the assumption that the bridge deck is symmetric (center of mass and elastic center overlap)

TABLE I
Section Model Parameters

Parameter	SmartBridge
Mass (m) [kg]	30.5
Mass moment inertia (I) [kgm^2]	1.02
Width excl. flaps (B') [mm]	500
Width incl. flaps (B) [mm]	740
Depth (D) [mm]	48
Length (L) [mm]	1800
Damping ratio pitch (ζ_α)	0.015
Damping ratio heave (ζ_h)	0.006
Circular natural frequency pitch (ω_α) [rad/s]	14.75
Circular natural frequency heave (ω_h) [rad/s]	11.85
Circular natural frequency flutter (ω_f) [rad/s]	12.95

the structural dynamics can be modeled as two uncoupled damped harmonic oscillators in heave and pitch [11].

The model of the external lift and moment caused by the aerodynamic forces on a canonical bridge section model can be estimated with Theodorsen's flutter derivatives [7].

The above described structural and aerodynamic models can be expressed with the following equations

$$M_s(\ddot{Y} + C_s\dot{Y} + K_sY) = C_{se}\dot{Y} + K_{se}Y \tag{1}$$

$$\begin{gathered} Y = \begin{bmatrix} h \\ \alpha \end{bmatrix}; \quad M_s = \begin{bmatrix} m & 0 \\ 0 & I \end{bmatrix} \\ C_s = \begin{bmatrix} 2\zeta_h\omega_h & 0 \\ 0 & 2\zeta_\alpha\omega_\alpha \end{bmatrix}; \; K_s = \begin{bmatrix} \omega_h^2 & 0 \\ 0 & \omega_\alpha^2 \end{bmatrix} \\ C_{se} = \tfrac{1}{2}\rho UBK \begin{bmatrix} H_1^* & BH_2^* \\ BAH_1^* & B^2A_2^* \end{bmatrix} \\ K_{se} = \tfrac{1}{2}\rho U^2K^2 \begin{bmatrix} H_4^* & BH_3^* \\ BAH_4^* & B^2A_3^* \end{bmatrix} \end{gathered} \tag{2}$$

where h and α are the heave and pitch positions, m is the mass of the deck, I is the mass moment of inertia of the deck, ζ_h and ζ_α are the damping ratios in the heave and pitch DOFs, and ω_h and ω_α are the natural circular frequencies in the heave and pitch DOFs. Furthermore, ρ is the air density, B is the bridge deck width, U is the wind speed, $K = B\omega/U$ is the reduced frequency, and $H_1^*, ..., H_4^*$ and $A_1^*, ..., A_4^*$ are the non-dimensional flutter derivatives for the deck. The flutter derivatives can be approximated with the values of a flat plate and are calculated with Theodorsen's circulatory function: $C(K) = F(K) + iG(K)$ [7], according to

$$\begin{gathered} H_1^*(K) = -\tfrac{2\pi F(K)}{K} \\ H_2^*(K) = -\tfrac{\pi}{2K}\left[1 + \tfrac{4G(K)}{K} + F(K)\right] \\ H_3^*(K) = -\tfrac{2\pi}{K^2}\left[F(K) - \tfrac{KG(K)}{4}\right] \\ H_4^*(K) = \tfrac{\pi}{2}\left[1 + \tfrac{4G(K)}{K}\right] \\ A_1^*(K) = \tfrac{\pi F(K)}{2K} \\ A_2^*(K) = -\tfrac{\pi}{8K}\left[1 - \tfrac{4G(K)}{K} - F(K)\right] \\ A_3^*(K) = \tfrac{\pi}{2K^2}\left[\tfrac{K^2}{32} + F(K) - \tfrac{KG(K)}{4}\right] \\ A_4^*(K) = -\tfrac{\pi G(K)}{2K}. \end{gathered} \tag{3}$$

When the bridge deck is at the point of flutter, the heave and pitch modes couple and oscillate with a constant amplitude at the same circular frequency, known as the flutter frequency, ω_f, and with a phase-shift, ϕ_f, between the two DOFs. This implies that the system in Eqs. 1 and 2 can be rewritten for the flutter condition as

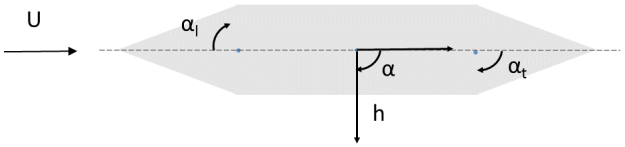

Fig. 3. Definitions of positive directions in the heave and pitch DOFs.

$$Y(t) = \begin{bmatrix} h_0 \\ \alpha_0 e^{-i\phi_f} \end{bmatrix} e^{i\omega_f t} \tag{4}$$

$$Y(t)\underbrace{\left[M_s(-\omega_f^2) + (C_s - C_{se})(i\omega_f) + (K_s - K_{se})\right]}_{\mathrm{A}} = 0. \tag{5}$$

The above two equations are thus only valid for the region of the flutter wind speed. Since the solution must be true for any non-zero $Y(t)$, the determinant of A has to be equal to zero in both real and imaginary parts.

The flutter condition is defined as the highest value of the reduced frequency, K, (i.e., the lowest wind speed U) where the following condition is met

$$\det(A) = 0. \tag{6}$$

C. Extended model for flap control

In order to consider the external lift and moment caused by the flaps, the model can be extended with a modified version of the wing-aileron-tab configuration (transformed into bridge deck with leading and trailing flaps) developed by Theodorsen and Garrick [8], an extension which implies additional flutter derivatives. The model is however only valid for the flutter condition and for flaps moving at the flutter frequency. Furthermore, it is assumed that the upwind elements do not influence the downwind elements and thus the bridge deck, the leading and trailing flaps force components can be superimposed.

In this paper, we investigate the amplitude-gain and phase-shift control law using the bridge deck's pitch as input, and the leading and trailing edge flaps' positions are calculated accordingly:

$$\alpha_l(t) = A_l e^{-i\phi_l}\alpha(t) \tag{7}$$

$$\alpha_t(t) = A_t e^{-i\phi_t}\alpha(t) \tag{8}$$

where A_l and A_t are the amplitude-gains, and ϕ_l and ϕ_t are the phase-shifts between the deck pitch and the leading and trailing edge flaps, respectively. The aerodynamic model can be extended to include the effects of the flaps by replacing H_2^*, H_3^*, A_2^* and A_3^* in Eq. 2 by $H_2^{*\prime}$, $H_3^{*\prime}$, $A_2^{*\prime}$ and $A_3^{*\prime}$ respectively. Specifically for the amplitude-gain and phase-shift control of the deck pitch, the modified flutter derivatives

are given by:

$$
\begin{aligned}
H_2^{*\prime} &= H_2^* + H_5^* A_t cos(-\phi_t) + H_6^* A_t sin(-\phi_t) \\
&+ H_7^* A_l cos(-\phi_l) + H_8^* A_l sin(-\phi_l) \\
H_3^{*\prime} &= H_3^* - H_5^* A_t sin(-\phi_t) + H_6^* A_t cos(-\phi_t) \\
&- H_7^* A_l sin(-\phi_l) + H_8^* A_l cos(-\phi_l) \\
A_2^{*\prime} &= A_2^* + A_5^* A_t cos(-\phi_t) + A_6^* A_t sin(-\phi_t) \\
&+ A_7^* A_l cos(-\phi_l) + A_8^* A_l sin(-\phi_l) \\
A_3^{*\prime} &= A_3^* - A_5^* A_t sin(-\phi_t) + A_6^* A_t cos(-\phi_t) \\
&- A_7^* A_l sin(-\phi_l) + A_8^* A_l cos(-\phi_l)
\end{aligned} \tag{9}
$$

where the additional flutter derivatives due to the flaps, $H_5^*, ..., H_8^*$ and $A_5^*, ..., A_8^*$, are given in the following equations:

$$
\begin{aligned}
H_5^*(K) &= \tfrac{1}{2K}\left[T_4 - F(K)T_{11} - \tfrac{4G(K)T_{10}}{K}\right] \\
H_6^*(K) &= \tfrac{1}{K^2}\left[-\tfrac{K^2 T_1}{4} - 2F(K)T_{10} + \tfrac{KG(K)T_{11}}{2}\right] \\
H_7^*(K) &= \tfrac{T_4}{2K} \\
H_8^*(K) &= -\tfrac{T_1}{4} \\
A_5^*(K) &= \tfrac{-T_1 + T_8 + cT_4 - \frac{T_{11}}{2} + \frac{F(K)T_{11}}{2} + \frac{2G(K)T_{10}}{K}}{4K} \\
A_6^*(K) &= \tfrac{-T_4 - T_{10} - \frac{K^2(T_7 + cT_1)}{4} + F(K)T_{10} + \frac{KG(K)T_{11}}{4}}{2K^2} \\
A_7^*(K) &= -\tfrac{T_1 - T_8 - cT_4}{4K} \\
A_8^*(K) &= \tfrac{1}{2K^2}\left[-T_4 - \tfrac{K^2}{4}(T_7 + cT_1)\right]
\end{aligned} \tag{10}
$$

where the values for the Theodorsen constants [8], $T_1, T_4, T_7, T_8, T_{10}$ and T_{11} are given in Table II.

By doing a parameter sweep of the control parameters, i.e., the amplitude-gains and the phase-shifts, we can analyze the effect that the control will have on the actively controlled bridge deck. In Fig. 4, the estimated flutter wind speed

TABLE II
THEODORSEN CONSTANTS

Constant	SmartBridge value
$c = B'/B$	0.676
$T_1(c)$	-0.0435
$T_4(c)$	-0.3303
$T_7(c)$	0.0106
$T_8(c)$	0.0899
$T_{10}(c)$	1.5654
$T_{11}(c)$	0.6840

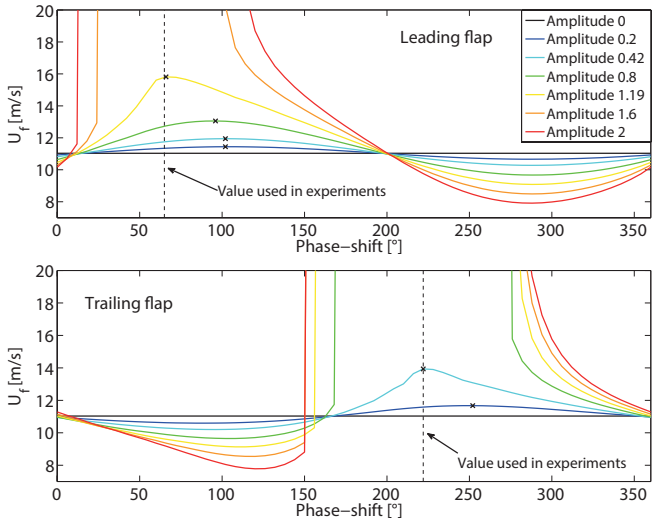

Fig. 4. Parameter sweep of the phase-shifts and amplitude-gains of the for the individual trailing and leading edge flaps.

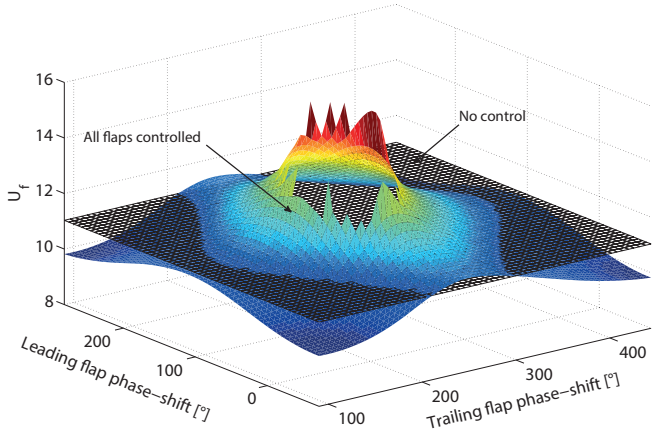

Fig. 5. The effect of the phase-shift parameter sweep when both flaps are controlled; the amplitude value is set to 0.35 here. The plane represents flutter wind speed of the bridge deck without control.

is presented for varying phase-shifts and amplitude-gains when controlling each side of the deck separately, thus only actuating flaps on one side of the deck at a time. The zero amplitude represents the flutter wind speed of the bridge deck without control, and is estimated to 11.0 m/s. It is observed that the optimal phase-shifts of the trailing and leading flap are dependent on the chosen amplitude-gains. Generally, the optimal phase-shift values seem to decrease with higher amplitude-gains. For the leading flap the optimal phase-shift is 102°when the amplitude-gain is 0.2, while it is 66°when the amplitude-gain is set to 1.19. Whereas for the trailing flap the phase-shift is optimal at 252°for an amplitude-gain of 0.2, while it is optimal at 222°when the gain is set to 0.42. Note that flutter does not even occur for a wide range of angles, when increasing the amplitude-gains further, as seen in Fig. 4 (for instance, for the leading flap control for a gain of 1.6 and phases-shifts between 24°and 102°). Furthermore, it is observed that increasing the amplitude-gains always increase the effect of the controller, for better

or for worse. Moreover, the trailing edge flap is capable of eliminating flutter at lower amplitude-gains than the leading edge flap, if optimal phase-shift parameters are chosen. These observations are also comparable to the theoretical analysis of Hansen et al. [4].

Furthermore, we analyzed the effect of controlling both flap arrays simultaneously, as can be seen in Fig. 5. Here, we analyze the flutter wind speed for different phase-shifts at a fixed amplitude-gain of 0.35 for all flaps. Observe that the flutter wind speed was increased but never completely eliminated when controlling the flaps separately at this amplitude-gain, as seen in Fig. 4. However, when the flaps on both sides are controlled simultaneously, their combined effect manage to also completely eliminate flutter (which is represented by the hole region on the surface). However, in a real scenario, other types of aerodynamic instabilities can occur at higher wind speeds that are not accounted for in our model, as has previously been pointed out by [3].

III. Wind Tunnel Experiments

The performance of the control laws were validated with wind tunnel experiments. The type of experiments performed, number of runs as well as the implemented control parameters can be found in Table III. An amplitude-gain of two should, according to our analytical study, be capable of eliminating flutter for a rather wide range of phase-shift values. We chose the phase-shift values that were close to the optimal (for the highest observable amplitude-gain) found in theory for the individual flap control, as seen in Fig. 4.

As a reference point, we observed from the wind tunnel experiments the deck without control fluttering at 12.5 m/s. This value is comparable to the estimated wind speed from the theoretical model, 11.0 m/s. The observed discrepancy is likely due to roughly approximated model parameters (e.g., the theoretical flutter derivatives are valid for flat plates).

The performance of the control of the bridge deck using all the flaps is visualized in Fig. 6. The control laws were triggered when any of the displacement sensors (placed at the corners of the deck) was oscillating with an amplitude above 40 mm. Note that the wind was turned off manually during the experiment without control, otherwise the self-induced vibrations of the flutter could damage the deck. It is also clear from the figure that the control is capable of suppressing the flutter (i.e., deter the development of self-induced vibrations). Furthermore, the flutter remained suppressed as the wind speed was increased to the upper bound of 16 m/s.

The performance of the different control algorithms, using all flaps, using only leading edge flaps, and using only trailing edge flaps, are presented in Fig. 7 and in Fig. 8. The qualitative difference between the three laws are visualized in Fig. 7, where it is clear that using all flaps for the control is more efficient than using flaps on a single edge. However, there does not seem to be a significant difference between using only flaps on the leading edge or only on the trailing edge.

Note that also the heave amplitude is more efficiently suppressed when using all the flaps, although this DOF is not

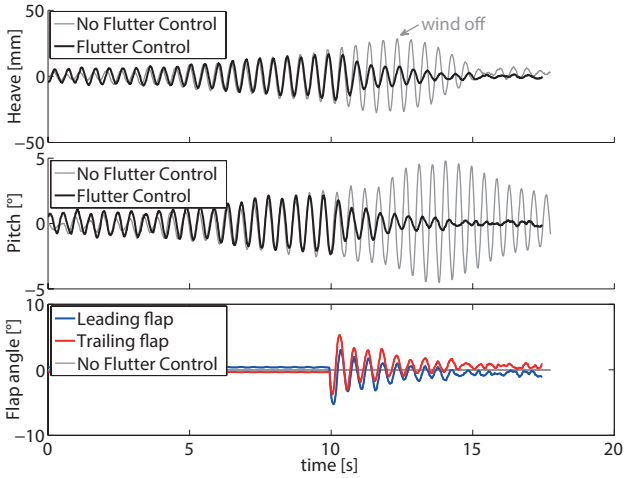

Fig. 6. The control using all flaps on the deck is compared to the deck without actively controlled flaps.

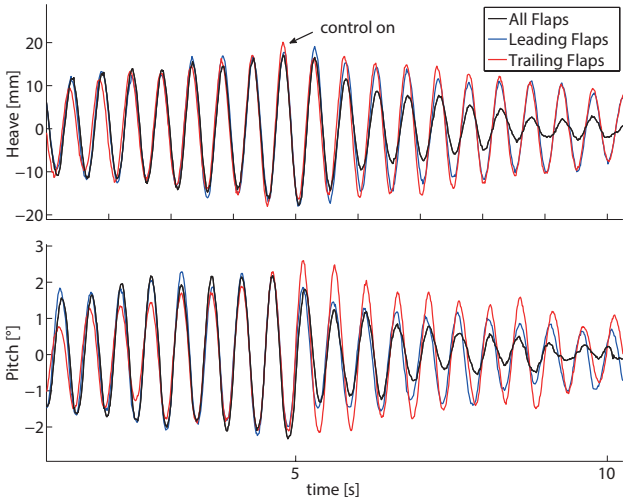

Fig. 7. The heave and pitch of the deck for the different control strategies. Note that the control is triggered at approximately 5 seconds.

actively controlled. The qualitative analysis is also supported by the performance comparison over all runs, including the uncontrolled case, in Fig. 8. The performance metric was defined as the damping ratio of the bridge pitch estimated from the 5 seconds following the control being triggered (in the case of no control, the point were the control would have been triggered was identified from the displacement sensor data). For the uncontrolled case the damping ratio is negative due to the growing amplitude during flutter. It is shown that the control strategy using all flaps is both performing better and with a smaller variance, than the other strategies. Again, no significant advantage for using either leading or trailing edge flaps when only one side is controlled can be seen, although, a strategy based on the leading edge flap appears to be more repeatable (smaller variance). Theoretically the trailing edge flap should be more efficient (assuming at least close to optimal phase-shift values), as seen in Fig. 4. This reverse relation could

TABLE III
WIND TUNNEL EXPERIMENTS

Flaps used in Control	Nr of experiments	Parameter	Value
None	1	ϕ_l	65
All flaps	10	ϕ_t	222
Leading edge flaps	10	A_l	2
Trailing edge flaps	10	A_t	2

be explained either by a non-optimal phase-shift value for the trailing edge, and/or an inadequate analytical model. As seen in Fig. 4, the phase-shift implemented in the control has a significant impact, although there is no guarantee that optimal parameters were used in the experiments. The model assumption that upwind elements do not influence downwind elements is quite improbable. Thus another explanation for the unexpectedly good performance of the leading edge flap could be that the altered flow over the deck and trailing flap has non-considered positive effects on the system damping.

In summary, we can with certitude assess that all three control laws lied within the "positive region" predicted by the model and that controlling the bridge deck using flaps on both sides is more effective (in terms of damping ratio) than using only flaps on a single side. This is a rather intuitive notion, however, an active flutter control of a bridge deck using both trailing and leading edges has, to the best of the authors' knowledge, not been studied experimentally before.

IV. CONCLUSIONS

In this paper, we investigated active flutter control of a bridge section model. The amplitude-gain and phase-shift control based on the bridge deck's pitch have been investigated in theory and with wind tunnel experiments. Three different strategies were compared; using all flaps available on both sides of the deck, and using only flaps on a single side of the deck, either on the leading or trailing edge. All of the proposed strategies proved capable, both theoretically and experimentally, of suppressing flutter. Moreover, it was shown that using all of the available flaps is the most efficient and reliable strategy, in theory as well as in practice. However, we did observe a discrepancy between theory and real experiments regarding the performance using only the trailing flaps and using only the leading flaps. In theory the trailing flaps should perform better than the leading flaps, while in practice they have a similar performance.

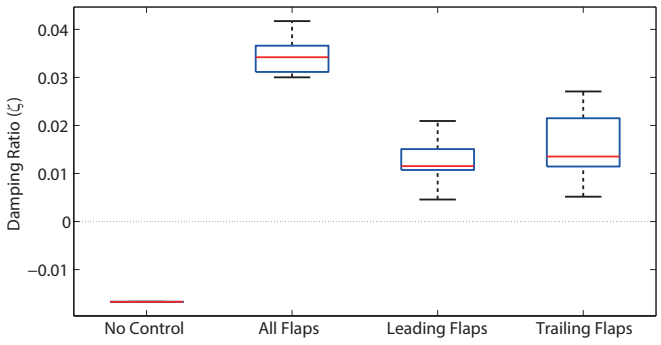

Fig. 8. Boxplot of the pitch damping ratios after 5 seconds of control for the four control strategies.

The analytical model was proven a useful tool in order to locate the regions where the control phase-shifts should be most efficient. However, the flutter wind speed prediction could be improved, for instance by extracting the flutter derivatives from the experimental set-up, instead of using theoretical approximations for flat plates.

The next step will be to leverage the gained knowledge of the model and control in the two dimensions, and implement coordinated control strategies also in the third dimension, thus controlling all of the eight flaps on the SmartBridge individually.

REFERENCES

[1] A. Larsen, *Aerodynamics of Large Bridges*. Taylor & Francis, 1992.

[2] H. Kobayashi and H. Nagaoka, "Active control of flutter of a suspension bridge," *Journal of Wind Engineering and Industrial Aerodynamics*, vol. 41, no. 1–3, pp. 143–151, 1992.

[3] H. Kobayashi, R. Ogawa, and S. Taniguchi, "Active flutter control of a bridge deck by ailerons," in *Second World Conference on Structural Control*, 1998, pp. 1841–1848.

[4] H. I. Hansen and P. Thoft-Christensen, "Active vibration control of long suspension bridges," Ph.D. dissertation, Aalborg University, 1998.

[5] H. I. Hansen, P. Thoft-Christensen, P. A. Mendes, and F. A. Branco, "Wind-tunnel tests of a bridge model with active vibration control," *Structural Engineering International*, vol. 10, no. 4, pp. 249–253, 2000.

[6] X. Zhao, K. Gouder, D. Limebeer, and J. Graham, "Experimental flutter and buffet suppression of a sectional suspended-bridge," in *Proceedings of the 53rd IEEE Conference on Decision and Control*, December 2014.

[7] T. Theodorsen, "General theory of aerodynamic instability and the mechanism of flutter," *NACA Tech. Rep. no. 496*, 1935.

[8] T. Theodorsen and I. E. Garrick, "Nonstationary flow about a wing-aileron-tab combination including aerodynamic balance," *NACA Tech. Rep. no. 736*, 1942.

[9] M. Boberg, G. Feltrin, and A. Martinoli, "Model and control of a flap system mitigating wind impact on structures," in *Robotics and Automation (ICRA), 2014 IEEE International Conference on*, May 2014, pp. 264–269.

[10] ——, "A novel bridge section model endowed with actively controlled flap arrays mitigating wind impact," in *Robotics and Automation (ICRA), 2015 IEEE International Conference on*, May 2015, pp. 1837–1842.

[11] E. Simiu and R. H. Scanlan, *Wind Effects on Structures: Fundamentals and Application to Design*. New York: John Wiley & Sons, 1996.